



HAL
open science

Atomistic description of phenol, CO and H₂O adsorption over crystalline and amorphous silica surfaces for hydrodeoxygenation applications

Youssef Berro, Saber Gueddida, Sébastien Lebègue, Andreea Pasc, Nadia Canilho, Mounir Kassir, Fouad El Haj Hassan, Michael Badawi

► To cite this version:

Youssef Berro, Saber Gueddida, Sébastien Lebègue, Andreea Pasc, Nadia Canilho, et al.. Atomistic description of phenol, CO and H₂O adsorption over crystalline and amorphous silica surfaces for hydrodeoxygenation applications. *Applied Surface Science*, 2019, 494, pp.721-730. 10.1016/j.apsusc.2019.07.216 . hal-02560240

HAL Id: hal-02560240

<https://hal.science/hal-02560240>

Submitted on 25 Oct 2021

HAL is a multi-disciplinary open access archive for the deposit and dissemination of scientific research documents, whether they are published or not. The documents may come from teaching and research institutions in France or abroad, or from public or private research centers.

L'archive ouverte pluridisciplinaire **HAL**, est destinée au dépôt et à la diffusion de documents scientifiques de niveau recherche, publiés ou non, émanant des établissements d'enseignement et de recherche français ou étrangers, des laboratoires publics ou privés.



Distributed under a Creative Commons Attribution - NonCommercial 4.0 International License

Atomistic description of phenol, CO and H₂O adsorption over crystalline and amorphous silica surfaces for hydrodeoxygenation applications

Youssef Berro,^{a,c} Saber Gueddida,^a Sébastien Lebègue,^{a,} Andreea Pasc,^b Nadia Canilho,^b*

Mounir Kassir,^c Fouad El Haj Hassan,^c Michael Badawi^{a,}*

^a Laboratoire de Physique et Chimie Théoriques LPCT UMR CNRS 7019, Université de Lorraine, Vandœuvre-lès-Nancy, France.

^b Laboratoire Lorrain de Chimie Moléculaire L2CM UMR CNRS 7053, Université de Lorraine, Vandœuvre-lès-Nancy, France.

^c Plateforme de Recherche et d'Analyse en Sciences de l'Environnement PRASE, Université Libanaise, Hadath, Liban.

* **Corresponding Authors:** sebastien.lebegue@univ-lorraine.fr ; michael.badawi@univ-lorraine.fr

KEYWORDS: HDO; Density Functional Theory; water; quartz; cristobalite; mesoporous silica;

Abstract

The upgrading of lignin-derived bio-oils involves a HydroDeOxygenation (HDO) reaction through either the Hydrogenation (Hyd) or the Direct DeOxygenation (DDO) route, the latter limiting hydrogen consumption. Herein, dispersion-corrected DFT has been used to evaluate the adsorption behavior of phenol (as a representative model of bio-oils) and two by-products (water and CO) over various crystalline and amorphous silica surfaces to evaluate their potential selectivity (DDO/ Hyd) and efficiency (low inhibiting effect) for HDO processing. Phenol can adsorb through three modes, flat π -interaction, flat O-interaction or perpendicular O-interaction. All crystalline surfaces show a preference for the flat π -interaction, which is expected to promote the Hyd route. Over amorphous surfaces the flat O-interaction dominates, and a very specific and strong interaction (around -120 kJ/mol) was found on SiO₂-3.3 and SiO₂-2.0 surfaces where the phenol molecule loses its aromaticity, which is very promising for its degradation under catalytic conditions. In addition, this makes those surfaces very efficient to adsorb selectively phenol in presence of water and CO. Remarkably, on all silica surfaces, the interaction energy of CO is nearly negligible, which makes them more attractive for HDO process compared to sulfide catalysts with respect to the inhibiting effect criteria.

1. Introduction

Hydrocarbons derived from lignocellulosic biomass have gathered an increasing interest for fuel production as they are respectful of environmental norms on CO₂ emissions [1–3]. Lignin consists of aryl ether units connected by ether and alkyl bonds, and the cleavage of those bonds yields to monomeric phenols and methoxyphenols [4]. Thus, bio-oils obtained by the pyrolysis of lignin contain a large number of phenolic compounds, up to 30% of the total oxygenated compounds, which represent 45 wt.% of the fraction. The other oxygenates present multiple functions such as aromatics, aldehydes, ketones, esters, acids, and alcohols.

A high oxygen content leads to deleterious properties such as thermal and chemical instability, high viscosity and poor engine efficiency [5–8]. Those bio-oils can be upgraded by HydroDeOxygenation (HDO), a thermal catalytic reaction under hydrogen pressure, to obtain oxygen-free molecules (aromatics or/and cycloalkanes) and water as the main by-product. It appears that phenolic compounds like guaiacol and alkylphenols are the most refractory compounds to the HDO process [9]. Therefore, in addition to studies devoted to the HDO of real feeds [10–13], the majority of research efforts are dedicated to the catalytic conversion of phenolic model molecules [14] such guaiacol and its derivatives [15–19]. Beside experimental studies, Density Functional Theory (DFT) calculations were used also to study the adsorption of oxygenated compounds and the competition of inhibiting molecules on catalytic sites present under HDO conditions [20–25].

These experimental and theoretical studies have shown that phenolic compounds follow two main deoxygenation routes: (i) the hydrogenation route (Hyd), which consists of the hydrogenation of the benzene ring into cyclohexyl before C-O bond cleavage or (ii) the direct deoxygenation (DDO) route where the C-O bond is directly broken, which limits the

consumption of hydrogen [14–16,26,27]. Excessive hydrogen consumption during the HDO reaction via the Hyd route increases the operating costs. Those costs are due to the use of large H₂ storage and pressurizing equipment, in addition to high H₂ and electricity consumption [13]. Therefore, the development of catalysts that enhance the DDO pathway is actively sought. Besides being selective towards the DDO pathway, a suitable HDO catalyst must meet other criteria such as a high activity, a good stability (*i.e.* no or limited deactivation), resistance to the inhibiting effect of the by-products, H₂O [28,29] and CO [26,30], and sustainability for environmental purposes.

Several catalysts and supports have been investigated extensively experimentally and theoretically in this field, including sulfides and metals [11–14,19,27–33]. Conventional sulfides CoMo and NiMo catalysts show promising performances following the DDO route [5,16,27]. However, their main drawback is the necessity to add H₂S in the feed to prevent catalyst oxidation [21,34,35]. In addition, H₂S can poison the active sites leading to a strong deactivation of the catalysts [26,28,35]. Sulfide catalysts are also sensitive to water [29] and carbon monoxide [26,30] under HDO conditions. Noble metals showed a high activity but are expensive and have a low selectivity toward aromatics [13,19,33]. Olcese et al. [18,36,37] studied the competition between DDO and Hyd routes using non-noble metals (Fe and Co) and showed that Fe/SiO₂ presents an interesting selectivity toward the DDO pathway. They proposed that the metallic reduced iron particles promote the dissociation of H₂, and then the H atoms react with the phenolic molecules adsorbed on the silanol groups of the silica surface [36]. The adsorption mechanisms of phenolic bio-oil molecules on different supports were studied by Popov et al. [38], showing that silica is more suitable for this purpose compared to alumina and silica-alumina supports.

Several DFT and combined DFT/experimental studies were done by Badawi et al. [20–22,30] in order to study the adsorption of oxygenated bio-oils and inhibiting competitive molecules (H₂S, water, and CO) over MoS₂ and CoMoS catalysts under HDO conditions. Those studies enlightened the main reason of the deficiency and deactivation of sulfided catalysts which is the very high competitive adsorption of water and CO. Using Density Functional Theory at finite temperature, Mian et al. [39] investigated the adsorption of catechol on the hydrophilic (001) cristobalite silica surface, having geminal silanol sites, in presence of competitive water molecules, and they concluded that catechol molecules displace preadsorbed water molecules and adsorb on the surface with a binding energy of -96 kJ/mol. Simonetti et al. [40] admitted the nomination of “parallel” and “perpendicular” when examining the adsorption modes of 5-fluorouracil on β -cristobalite surface. They identified the H-bonding interactions between the molecule and the surface silanols, and proved their effect on stabilizing the molecule on the silica surface. They also discussed the occurrence of π -interaction (between the aromatic ring and the silanol group) in the “parallel” adsorption [40,41], in accordance with Rimola et al. [42] results on benzene-silanol interactions. Other molecules have been studied showing the importance of the H-bonding interactions, induced by the existence of silanols on the silica surface, in controlling drug delivery [43,44]. Inspired by those previous works in HDO field as well as by similar studies on the adsorption modes during the HydroDeSulfurization HDS of thiophene [45–47] we investigated herein two main adsorption modes: (1) perpendicular O-interaction of phenol (perp O-int) vs (2) flat π -interaction (flat π -int) on silica surface. The phenol perp O-int adsorption mode is expected to favor the DDO route and to produce benzene as a major product, while the phenol flat π -int adsorption mode is expected to favor the Hyd route and to produce cyclohexanol that deoxygenate to give cyclohexane as a major product (see **Figure 1**).

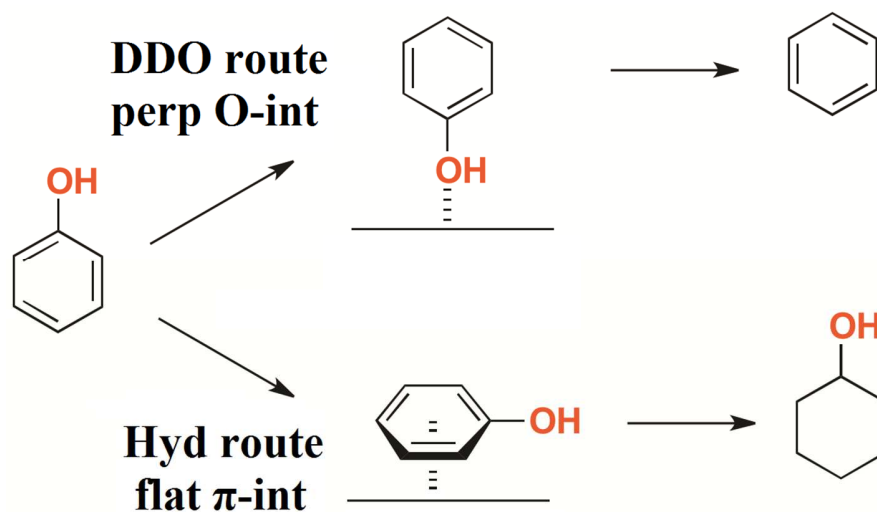


Figure 1. Phenol adsorption mechanisms over silica surface: perpendicular O-interaction (perp O-int) promoting the DDO route vs flat π -interaction (flat π -int) promoting the Hyd route.

Despite the fact that previous studies showed promising performance of silica-supported catalysts in HDO processing [13,18,19,37,38], the adsorption mechanisms and energies of phenolic molecules and by-products such as H₂O and CO over different sites of various possibly used silica surfaces for the HDO application have not been studied yet. Here, the adsorption energies of phenol (as a representative model of bio-oil vapors) and the by-products (water and CO) are computed by DFT calculations over different crystalline and amorphous silica structures in order to identify the most efficient surface that favors perp O-int (therefore expected to promote the DDO route) and bears the lowest inhibiting effect of the by-products. The present study is organized as follows: first, we will present the silica models used in this work, including crystalline surfaces ((111), (101), (001) β -cristobalite, and (001) α -quartz) and amorphous surfaces [48] (with a silanols density ranging from 1.1 to 7.2 OH/nm²). Then, the DFT methods and parameters, and the calculation method of the adsorption energies are described. After, we will present the results of the phenol adsorption following different modes and the potential promotion of the DDO or the Hyd routes attached to each mode. Then, the inhibiting effect of

water and CO on the adsorption of phenol over all silica surfaces is interpreted. From those results and experimental conditions, a conclusion is deduced on the most appropriate surface that would promote the DDO route with less competition of inhibiting molecules.

2. Materials and methods

2.1 Models of Silica Surfaces

2.1.1 β -cristobalite Surfaces

In order to build our models, we used the bulk geometry of SiO₂ that was previously relaxed in the tetragonal $I\bar{4}2d$ space group [49,50]. Surfaces are modeled by slabs, constructed by cutting the bulk crystal along the (111), (101) and (001) crystallographic planes. The surfaces are terminated by oxygen atoms which are saturated with hydrogen, hence forming hydroxyl-group-covered surfaces (–OH), which are representative of the energetically most stable SiO₂ surfaces [50].

Three layers of [111], [101] and [001] silica surfaces having isolated silanols with a density of 4.29 OH/nm², 5.24 vicinal sites per nm² and 7.42 geminal sites per nm², respectively, were constructed. The two bottom layers are frozen in the geometry of the bulk and the top layer is free to relax. The [111] surface unit cell (**Figure 2.a**) is composed of 96 Si, 208 O, and 32 H atoms with $a = 20.26$, $b = 20.57$, $c = 31.54$ Å (including 15 Å of vacuum). The [101] surface (**Figure 2.b**) unit cell is composed of 80 Si, 176 O, and 32 H atoms, while the [001] surface (**Figure 2.c**) is composed of 64 Si, 144 O, and 32 H atoms.

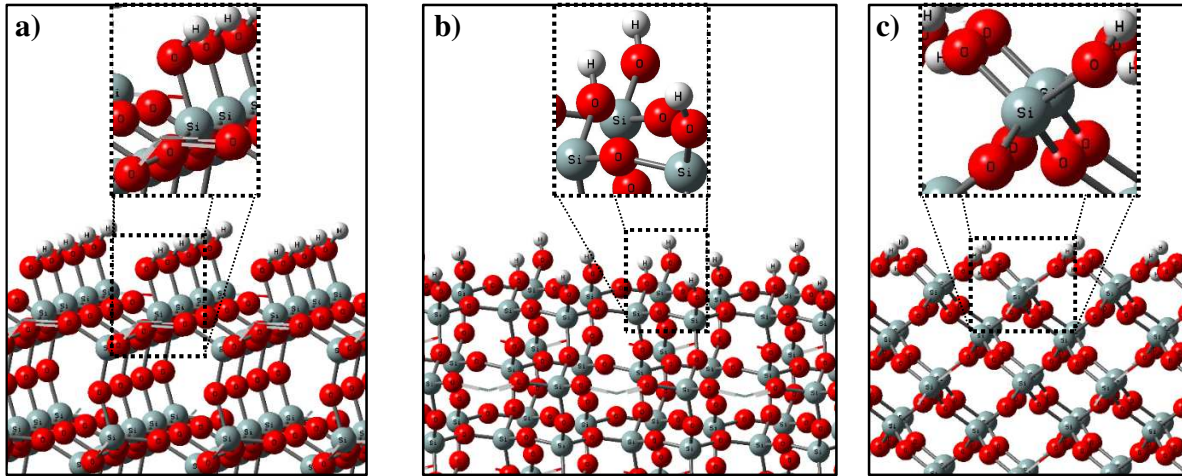


Figure 2. **a)** [111] β -cristobalite unit cell with isolated silanols (4.29 OH/nm²), **b)** [101] β -cristobalite unit cell with vicinal silanols (5.24 OH/nm²), and **c)** [001] β -cristobalite unit cell with geminal silanols (7.42 OH/nm²).

2.1.2 [001] α -quartz Surface

Periodic DFT studies of the cleaved, reconstructed and fully hydroxylated [001] α -quartz surfaces at various thickness have been performed by Goumans et al. [51] The surface investigated herein is the fully hydroxylated one used also by Abbasi et al. [52] with 8.28 OH/nm² of geminal, H-bonded to each other's, silanols. The studied surface, shown in **Figure 3**, is constructed using a SiO₂ slab in a tetragonal supercell 14.74*14.74*25 Å³ (including 10 Å of vacuum) and composed of 36 H, 126 O, and 54 Si atoms.

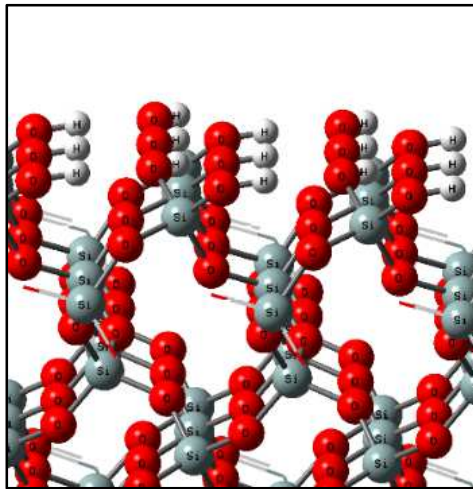


Figure 3. Fully hydroxylated [001] α -quartz silica surface with 8.28 geminal OH/nm².

2.1.3 Amorphous Surfaces

Amorphous surfaces are notoriously difficult to handle with periodic calculations. Here, we use some of the geometries constructed by Comas-Vives [48] via the dehydroxylation of a fully hydroxylated surface. The amorphous silica structures having a silanols density of 7.2, 5.9, 4.6, 3.3, 2, and 1.1 OH/nm² were chosen as a representative sample, and labelled SiO₂-7.2, SiO₂-5.9, SiO₂-4.6, SiO₂-3.3, SiO₂-2.0, and SiO₂-1.1 respectively. **Figure 4** shows the fully hydroxylated SiO₂-7.2 (**Figure 4.a**) and fully dehydroxylated SiO₂-1.1 (**Figure 4.b**) amorphous surfaces. Five silanol group types (isolated, vicinal, geminal, nest-1, and nest-2) are present on the SiO₂-7.2 fully hydroxylated surface, while only isolated silanols are present on the SiO₂-1.1 fully dehydroxylated surface.

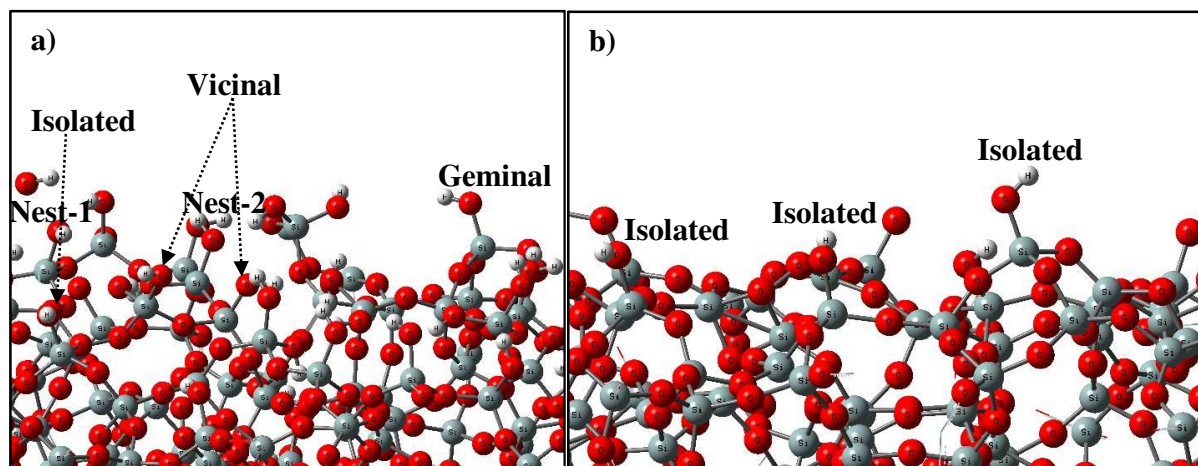


Figure 4. a) Amorphous $\text{SiO}_2\text{-7.2}$ (7.2 OH/nm^2) surface with various silanol groups, b) Amorphous $\text{SiO}_2\text{-1.1}$ (1.1 OH/nm^2) surface with only isolated silanol groups.

2.2 Computational Methods

Periodic DFT calculations [53,54] have been performed using the Vienna Ab initio Simulation Package (VASP) [55,56], where the electronic wave functions have been expanded into plane waves up to a 450 eV cut-off energy. The semi-local Perdew–Burke–Ernzerhof (PBE) exchange-correlation functional in the generalized gradient approximation (GGA) proposed by Perdew et al. [57] was chosen. The projector augmented wave (PAW) method [58,59] was used to describe the electron-ion interactions and the Kohn-Sham equations were solved self-consistently until the energy difference between cycles decreases below 10^{-6} eV. A Gaussian smearing of $\sigma = 0.1$ eV was applied to band occupations in order to improve the total energy convergence. The atomic positions have been relaxed until all forces were smaller than 0.03 eV/\AA per atom. The Γ -point was used for the Brillouin zone integration.

The importance of dispersion forces on DFT calculations for similar adsorption applications where adsorbates are very close to the surface was highlighted by Sun et al. [60]. Therefore, Van der Waals (vdW) interactions have been taken into account [61–65] to describe the long-range electron correlation that contributes significantly to the adsorption process. A computationally

affordable approach consist in adding a pairwise interatomic C_6R^{-6} term to the DFT energy [66–71]. Here, the semi-empirical D2 approach of Grimme [68,69] is adopted. In **Supporting Information**, we will present the effect of dispersion (vdW) forces on the adsorption energies of studied molecules over crystalline surfaces, in order to highlight the importance of taking into account those interactions.

Several sets of DFT calculations have been conducted, the first considers the relaxation of the first layer of the silica structure (with the bottom fixed) and enable us to obtain the energy of pure silica surface $E_{\text{SiI,DFT}}$. The second set enables determining the energies of isolated molecules water, CO, and phenol in the gaseous phase $E_{\text{X,DFT}}$ (where all atoms are relaxed). The third is a geometrical optimization of the interaction of those molecules on the silica surface, giving $E_{\text{SiI-X,DFT}}$ (the molecules and the first silica layer are relaxed). From those energies, we calculate the adsorption energies $E_{\text{ads,DFT}}$ between molecules and the silica surface as follow:

$$E_{\text{ads,DFT}} = E_{\text{SiI-X,DFT}} - E_{\text{SiI,DFT}} - E_{\text{X,DFT}}$$

3 Results and discussion

3.1 Phenol Adsorption Modes on Silica Surfaces

The type and the number of interacting silanol groups with the phenol molecule affect the adsorption mode. On one hand, the perp O-int adsorption mode, that is expected to promote the DDO route, includes usually the interaction of the oxygen atom of phenol with the hydrogen atom of the silanol group (H-bond acceptor, $\text{PhOH} \cdots \text{HO-Si}$) and/or the interaction of the hydrogen atom of phenol with the oxygen atom of the silanol group (H-bond donor, $\text{PhOH} \cdots \text{HO-Si}$). On the other hand, the flat π -int adsorption mode, that would favor the Hyd route, is induced principally by the interaction of the phenol ring with the OH of the silanol

group (π -interaction, HO-Ph(π) \cdots HO-Si), but it may include the H-bond donor and H-bond acceptor interactions types. The third adsorption mode, flat O-int, is found over amorphous surfaces where the phenol molecule interacts with the surface through its hydroxyl group (H-bond donor or/and acceptor), which would be to the advantage of the DDO route. However, the aromatic ring is parallel to the surface and would be close enough to promote also the Hyd route (Figure 5).

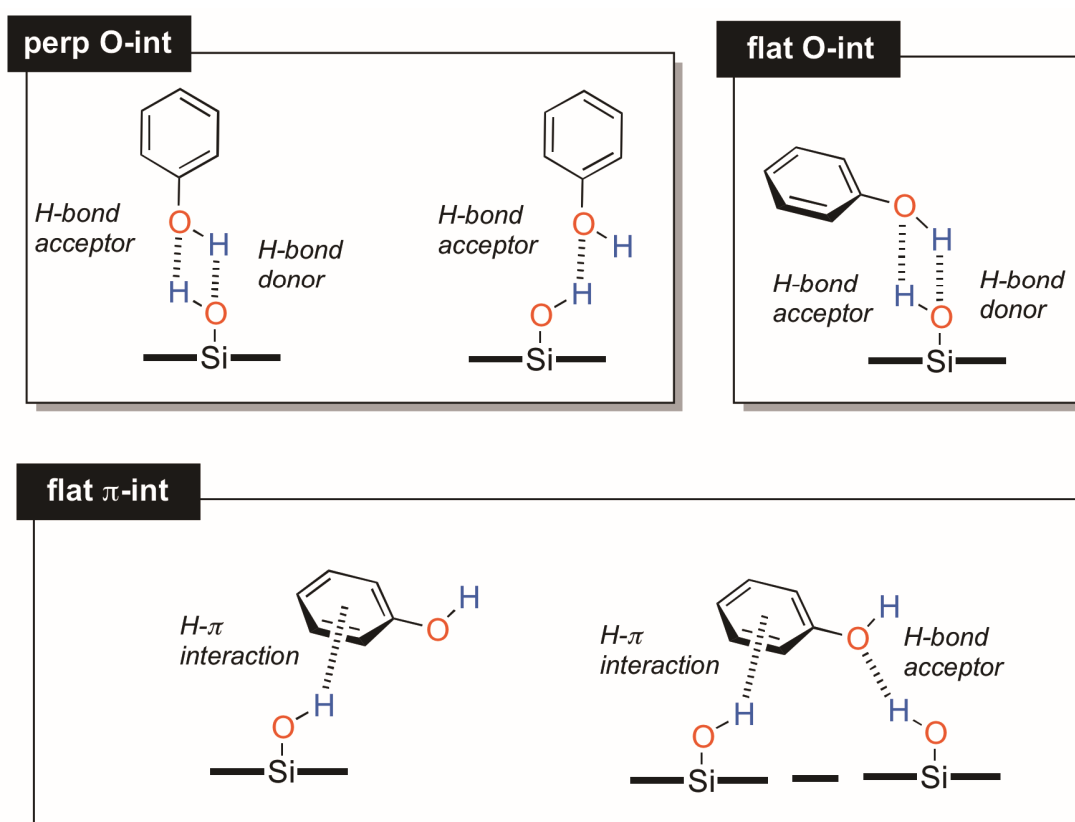


Figure 5. The possible types of interaction (H-bond donor, H-bond acceptor, and π -interaction) occurring during the adsorption of phenol via the three modes perp O-int, flat π -int, and flat O-int over silica surfaces.

3.1.a Crystalline Silica Surfaces

Two possible phenol adsorption mechanisms (perp O-int and flat π -int) have been identified over the [001], [101], [001] β -cristobalite surfaces, and [001] α -quartz surfaces (Figure 6). The

adsorption energies of phenol in both modes over the various crystalline surfaces are compared in **Figure 7**. Results show that the [101] β -cristobalite surface, having vicinal silanols, favors equally the perp O-int and the flat π -int modes in comparison to other crystalline surfaces where the flat π -int mode dominates.

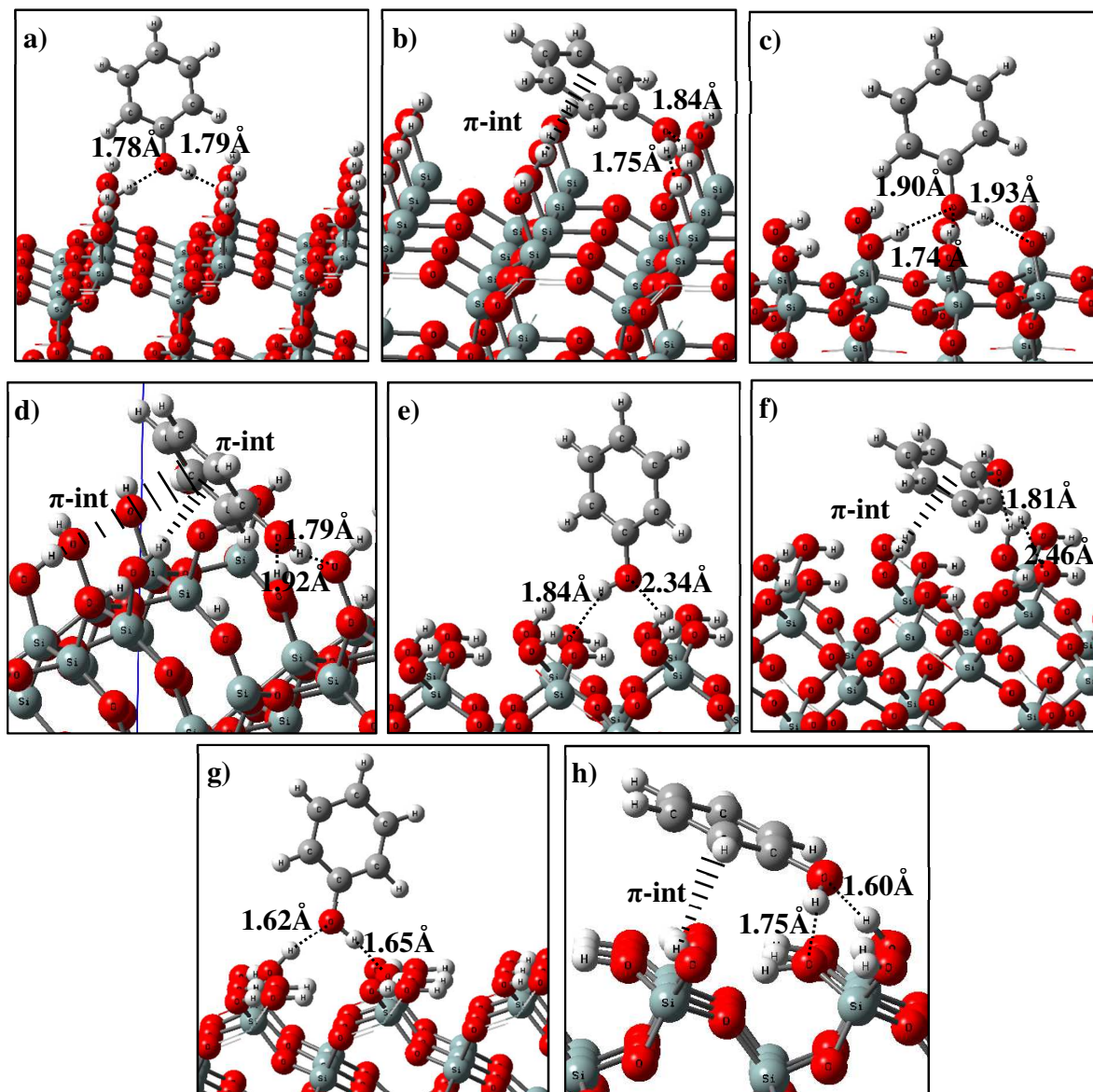


Figure 6. Phenol adsorption configuration modes over crystalline silica surfaces: **a)** perp O-int over [111] β -cristobalite, **b)** flat π -int over [111] β -cristobalite, **c)** perp O-int over [101] β -cristobalite, **d)** flat π -int over [101] β -cristobalite, **e)** perp O-int over [001] β -cristobalite, **e)** flat π -int over [001] β -cristobalite, **f)** perp O-int over [001] α -quartz, **h)** flat π -int over [001] α -quartz.

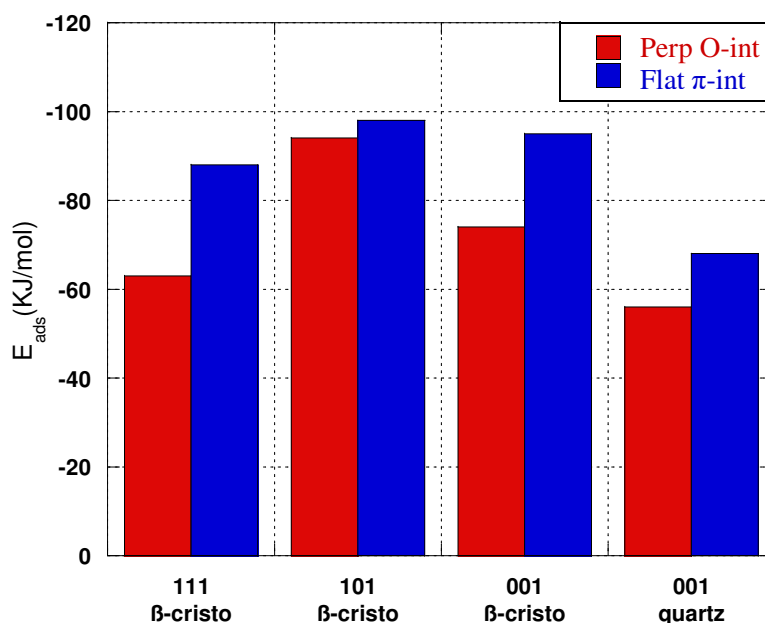


Figure 7. Adsorption energies of phenol (perp O-int vs flat π -int) over crystalline surfaces.

The interaction types and lengths between phenol molecule and silanol groups of different surfaces are presented in **Table 1**. The length of the interaction between the OH group of the phenol and the silanols varies from 1.60 to 2.05 Å depending on the silica surface (density and type of silanols). When comparing the phenol perp O-int with the flat π -int over the [101] β -cristobalite; it appears that the H-bond donor and acceptor interaction types present similar bonding lengths resulting in similar interactions. Another important geometrical parameter is the length of the C-O bond of the phenol molecule, the initial C-O bond length before interaction with silica surfaces being of approximately 1.40 Å. This length decreases to an average of 1.38 Å with no large variation depending on the adsorption mechanism and the silica surface. It is obvious that high adsorption energies correspond to phenol adsorption over silica surfaces having three interactions, while those having two interactions show an energy around -65 kJ/mol, and those with only one-interaction show lower energy values.

Table 1. Interaction types and distances between phenol and crystalline surfaces.

	perp O-int	flat π-int
[111] β-cristobalite	PhOH \cdots HO-Si: 1.82 Å	PhOH \cdots HO-Si: 2.05 Å
	PhOH \cdots HO-Si: 1.79 Å	PhOH \cdots HO-Si: 1.76 Å
	-	HO-Ph(π) \cdots HO-Si
[101] β-cristobalite	PhOH \cdots HO-Si: 1.92 Å	PhOH \cdots HO-Si: 1.92 Å
	PhOH \cdots HO-Si: 2.05 Å	PhOH \cdots HO-Si: 1.79 Å
	PhOH \cdots HO-Si: 1.82 Å	HO-Ph(π) \cdots HO-Si
[001] β-cristobalite	PhOH \cdots HO-Si: 1.71 Å	PhOH \cdots HO-Si: 2.00 Å
	PhOH \cdots HO-Si: 1.70 Å	PhOH \cdots HO-Si: 1.74 Å
	-	HO-Ph(π) \cdots HO-Si
[001] α-quartz	PhOH \cdots HO-Si: 1.60 Å	PhOH \cdots HO-Si: 1.60 Å
	-	PhOH \cdots HO-Si: 1.75 Å
	-	HO-Ph(π) \cdots HO-Si

3.1.b Amorphous Silica Surfaces

Figure 8 shows the adsorption modes of phenol on various amorphous silica surfaces as a function of the silanol type and densities. Adsorption energies of phenol corresponding to various interaction modes (perp O-int, flat π -int, and flat O-int) over all considered sites of silica surfaces are compared in **Table 2**.

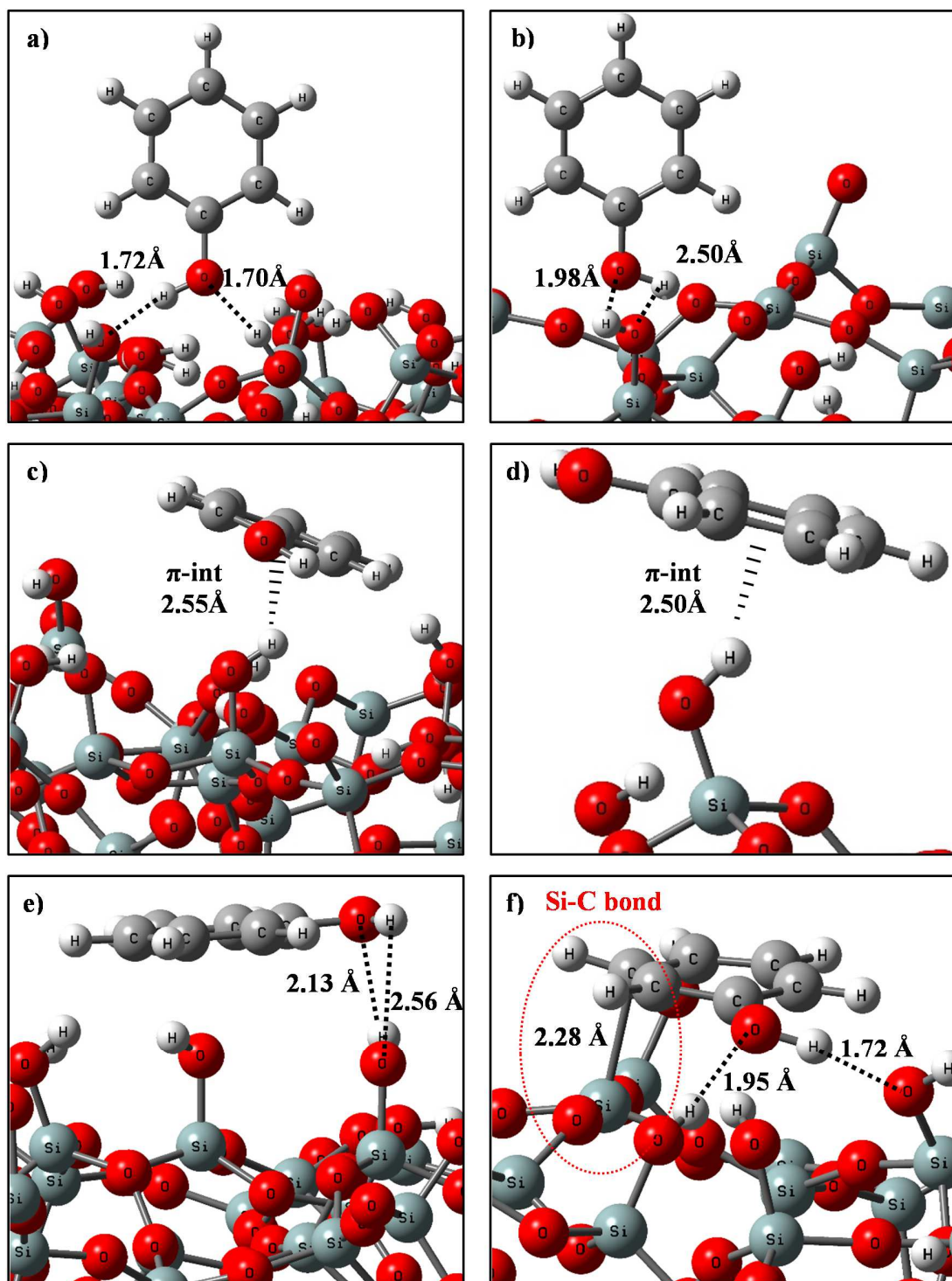


Figure 8. Adsorption mechanisms of phenol over different sites of various amorphous silica surfaces: **a)** perp O-int over nest-2 site of SiO₂-7.2, **b)** perp O-int over vicinal site of SiO₂-2.0, **c)** flat π-int over vicinal site of SiO₂-5.9, **d)** flat π-int over isolated site of SiO₂-1.1, **e)** flat O-int over nest-2 site of SiO₂-3.3, **f)** flat O-int over nest-1 site of SiO₂-2.0.

Based on the models of Comas-Vives [48], five types of silanols (isolated, nest-1, vicinal, nest-2, geminal) are present on the most saturated surfaces for 3.3 OH/nm² and higher. Nest 1 site is composed of a vicinal silanol and an isolated silanol while nest 2 is composed of a geminal silanol associated to one OH group of a neighbor vicinal silanol. For SiO₂-2.0, one can observe the disappearance of nest-2 and geminal sites. For the most unsaturated surface SiO₂-1.1, only isolated sites are present. If we compare the strength of adsorption sites per sites, the interaction of phenol with the silanols globally increase in the following order: isolated and vicinal (from -19 to 55 kJ/mol) < geminal (from -22 to -76 kJ/mol) < nest-2 (from -31 to -77 kJ/mol) < nest-1 (from -33 to -120 kJ/mol).

Table 2. Phenol adsorption energies (kJ/mol) over different sites of amorphous surfaces with various silanol densities and types. The most favorable configuration for phenol adsorption is indicated in bold for each silanols density.

Silanols Site		Isolated	Nest-1	Vicinal	Nest-2	Geminal
SiO ₂ -7.2	perp O-int	-33	-54	-30	-65	-46
	flat π-int	-34	-59	-26	-45	-29
	flat O-int	-31	-34	-55	-70	-51
SiO ₂ -5.9	perp O-int	-26	-50	-29	-51	-27
	flat π-int	-22	-46	-29	-31	-27
	flat O-int	-26	-52	-30	-35	-24
SiO ₂ -4.6	perp O-int	-19	-69	-23	-62	-76
	flat π-int	-42	-82	-33	-65	-43
	flat O-int	-27	-80	-19	-44	-58
SiO ₂ -3.3	perp O-int	-34	-54	-20	-73	-23
	flat π-int	-29	-33	-18	-42	-22
	flat O-int	-31	-117	-35	-77	-24
SiO ₂ -2.0	perp O-int	-19	-53	-21	*	*
	flat π-int	-22	-35	-17	*	*
	flat O-int	-30	-120	-38	*	*
SiO ₂ -1.1	perp O-int	-22	*	*	*	*
	flat π-int	-24	*	*	*	*
	flat O-int	-26	*	*	*	*

For the SiO₂-7.2 surface which presents the highest silanol density, the most favorable configuration for phenol adsorption is a flat O-int on the nest 2 (-70 kJ/mol), followed by a flat π -int on the nest 1 (-59 kJ/mol). For silanol density ranging from 2 to 5.9 OH/nm², the phenol always prefers to accommodate on the nest 1, via a flat O-int mode, except for SiO₂-4.6 where the flat O-int and flat π -int modes coexist (adsorption energy around -80 kJ/mol). In addition for this silanol density, phenol can adsorb quite strongly (-76 kJ/mol) on the geminal site through a perp O-int mode, which could favor the DDO route in HDO reaction.

For SiO₂-2.0 and SiO₂-3.3 surfaces, very high interaction energies (around -120 kJ/mol) are observed for nest 1, due to an optimal accommodation of the phenol molecule on the surface. For this configuration (**see Figure 8.f**), two hydrogen bonds are formed, one between the H atom of the hydroxyl group of phenol and the O atom of an isolated silanol (1.72 Å), the other between the O atom of phenol and the H atom of a vicinal silanol (1.95 Å). In addition, a deformation of the phenol structure (loss of its planarity corresponding to a destabilization around 20 kJ/mol compared to the molecule alone), is observed leading to a specific interaction between the aromatic ring and a Si atom of the surface (distance between this Si atom and the carbon γ of 2.28 Å). Similar adsorption configurations have been found in the literature for furan [20] and thiophene [45] on MoS₂ surfaces, which chemically activate the molecules. The interaction energy of phenol with the nest 1 progressively decreases when the silanol density increases, as the presence of additional silanol group(s) hinder or limit the interaction(s) described above. Finally, the SiO₂-1.1 weakly adsorb phenol (around -25 kJ/mol) without favoring any adsorption mode.

Phenol can be more adsorbed on amorphous silica surfaces than crystalline surfaces in general because of the presence of silanol nests on the amorphous surfaces which allows the phenol to interact through several hydrogen bonds, π -ring interaction and Si-C bonds at the same time. However, when comparing similar sites of both types of surface (namely geminal, vicinal and isolated silanols), we observe higher phenol adsorption energies over crystalline surfaces, due to the surrounding environment of the site and the morphology of the structure. For example, the adsorption energy of phenol on the isolated site for all the amorphous surfaces is around -30 kJ/mol, which is much smaller than the one found (-88 kJ/mol) over the [111] β -cristobalite surface (having only isolated silanols). This high value is due to the surrounding isolated silanols over the crystalline surface where the phenol molecule interacts with several isolated silanols, while over the amorphous surface the isolated site is really far from any other silanol.

Regarding the potential consequences on the reactivity of phenol upon HDO conditions, it is hard to conclude on the DDO or HYD selectivity as the flat O-int is the most favorable configuration for almost all amorphous silica surfaces. Only the SiO₂-4.6 shows a potential good HDO selectivity as it could favor the DDO route if phenol adsorbs on geminal sites. Further investigations such as the calculation of reaction mechanisms are needed to provide better conclusions, but they are beyond the scope of the present work. Nonetheless, one important feature of materials to be used in HDO processes is their ability to prevent inhibiting effect of by products on the adsorption of reactants, which will be developed in the next section.

3.2 Competitive Adsorption of Inhibiting Molecules

The competitive adsorption of inhibiting molecules (water and CO) is one of the main parameters that affect the hydrodeoxygenation process. A comparative histogram of adsorption energy of water, CO, and phenol onto crystalline silica surfaces is presented in **Figure 9**. The interaction energy of CO is low (around -20 kJ/mol) whatever the crystalline surface. As the energy of phenol adsorption is around -90 kJ/mol, the inhibition effect of CO is expected to be negligible. Those results suggest that silica-based materials are particularly promising for the HDO process comparing to conventional MoS₂ and CoMoS catalysts which suffer from a strong competitive adsorption of CO (CO interaction energy over CoMoS 50% M-edge is four times higher than that of phenol, with a value of -160 kJ/mol), in addition to the poisoning effect of H₂S [30].

Our computed water adsorption energies are similar to those calculated by Yang et al. [72] for [111] β -cristobalite (-77 kJ/mol compared to -74 kJ/mol) and [001] β -cristobalite (-42 kJ/mol compared to -43 kJ/mol). As well, similar adsorption energy is found over the [001] α -quartz as that reported by Yang et al. [73] (-58 kJ/mol compared to -53 kJ/mol). The competition between water and phenol cannot be considered minor, with an adsorption energy difference of about -10 kJ/mol, except on the [001] β -cristobalite surface. The water adsorption energy of those surfaces is much higher than the water liquefaction heat (-44 kJ/mol) that is usually used to define the hydrophobicity of the surface [74,75]. Therefore, the [111] β -cristobalite, [101] β -cristobalite and [001] α -quartz surfaces can be considered as hydrophilic, unlike the [001] β -cristobalite surface where the adsorption energy of water is around -42 kJ/mol.

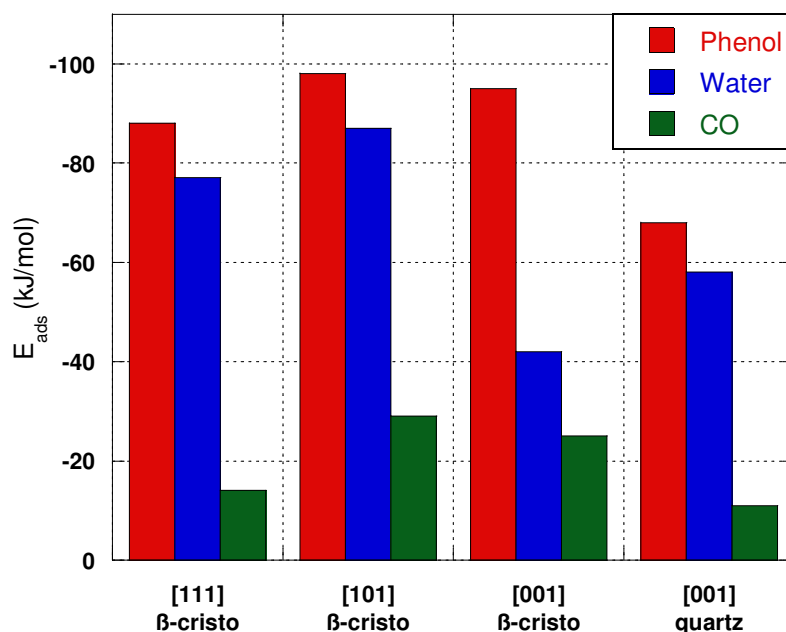


Figure 9. Adsorption energies of phenol and inhibiting molecules over crystalline surfaces.

The adsorption energies of phenol and inhibiting molecules on various sites of amorphous surfaces are gathered in **Table 3**. As for crystalline surfaces, CO is weakly adsorbed compared to phenol. Indeed, the CO adsorption energy over the more hydroxylated surface (SiO₂-7.2) is around -20 kJ/mol, and it is much smaller over other surfaces. The inhibiting effect of water on the adsorption of phenol is expected to be important for the most hydroxylated surfaces (SiO₂-7.2 and SiO₂-5.9) as the adsorption energy of water can exceed the one of phenol by 50 kJ/mol on some sites (as the isolated silanol). However, the effect of water becomes more and more limited when decreasing the silanol density, in line with the fact that amorphous surfaces having a silanol density larger than 5 OH/nm² can be considered hydrophilic ($E_{\text{ads}} > \text{heat of liquefaction}$). Over SiO₂-4.6, the adsorption energies of water and phenol are similar for every sites except the isolated one where phenol is more adsorbed than water by 22 kJ/mol. Remarkably, the adsorption of phenol is expected to be not impacted by the presence of water on the SiO₂-3.3 and SiO₂-2.0 surfaces as their nest-1 site can strongly interact with phenol (around -

120 kJ/mol), which is much larger than water on the same site (around -50 kJ/mol) or other sites (between -20 and -30 kJ/mol).

Table 3. Inhibiting molecules competition: Adsorption energies (kJ/mol) of water, CO, and phenol over different sites of amorphous surfaces.

Silanol Sites		Isolated	Nest-1	Vicinal	Nest-2	Geminal
SiO₂-7.2	Phenol	-34	-59	-55	-70	-51
	H₂O	-85	-67	-26	-74	-30
	CO	-18	-21	-18	-21	-19
SiO₂-5.9	Phenol	-26	-52	-30	-51	-27
	H₂O	-76	-55	-39	-58	-24
	CO	-8	-9	-14	-14	-11
SiO₂-4.6	Phenol	-42	-82	-33	-65	-76
	H₂O	-20	-81	-32	-63	-67
	CO	-10	-13	-12	-21	-13
SiO₂-3.3	Phenol	-34	-117	-35	-77	-24
	H₂O	-34	-51	-24	-70	-19
	CO	-11	-11	-11	-12	-7
SiO₂-2.0	Phenol	-30	-120	-38	*	*
	H₂O	-31	-55	-24	*	*
	CO	-14	-13	-11	*	*
SiO₂-1.1	Phenol	-26	*	*	*	*
	H₂O	-33	*	*	*	*
	CO	-13	*	*	*	*

4. Conclusion

The HydroDeOxygenation (HDO) reaction is a key step in the upgrading of lignin and occurs through either the Hydrogenation (Hyd) or the Direct DeOxygenation (DDO) route, the latter being highly desirable because it limits the hydrogen consumption. The selectivity (DDO route promotion) and the efficiency (low inhibiting effect of by-products) of the HDO reaction are strongly depending on the surface properties of the catalyst. Knowing that the adsorption is the first step of the catalytic mechanism, this study focuses on the adsorption properties of different

crystalline and amorphous silica surfaces. The adsorption energies of phenol via three interaction modes (perpendicular O-interaction, flat π -interaction, and flat O-interaction), and inhibitor molecules (water and CO) over silica surfaces are investigated and compared using dispersion-corrected DFT calculations. The flat π -interaction, where the phenol is parallel to the surface and interacts with it through its aromatic ring, dominates over all crystalline surfaces, which would favor the Hyd route. Over amorphous surfaces the flat O-interaction dominates, and a very specific and strong interaction (around -120 kJ/mol) was found on SiO₂-3.3 and SiO₂-2.0 surfaces where the phenol molecule loses its aromaticity, which is very promising for its degradation under catalytic conditions.

Furthermore, the competitive effect of inhibiting molecules (water and CO) is interpreted. We have shown that CO competition is negligible over all silica surfaces, which make them more attractive than conventional sulfide catalysts in respect with this criterion. The inhibiting effect of water on the adsorption of phenol is expected to be important for the amorphous surfaces having a silanol density higher than 5 OH/ nm². However, the SiO₂-3.3 and SiO₂-2.0 surfaces exhibit a very weak adsorption of water (and CO) compared to phenol. Our results should motivate the synthesis of amorphous silica having between 2 and 4 OH/nm² and further catalytic tests for HDO applications as they could present a highly selective adsorption of phenolic molecules towards by-products H₂O and CO.

Acknowledgments

Youssef Berro would like to thank the Lebanese University and the Lebanese National Council for Scientific Research CNRS-Lebanon for funding his Ph.D. The authors gratefully acknowledge Dr Anthony Dufour (CNRS, Université de Lorraine) for fruitful discussions and LUE Mirabelle+/project Lignin and PHC CEDRE Future Materials for financial support. HPC

resources provided by PMMS (Pôle Messin de Modélisation et de Simulation) and GENCI-CCRT/CINES (Grants No. A0040910433 and No. A0060910433) are acknowledged.

Appendix A. Supplementary data

Contains results and discussions regarding the contribution of dispersion forces (vdW interactions) to the overall interaction energies of phenol, CO and water over crystalline and amorphous silica surfaces.

References

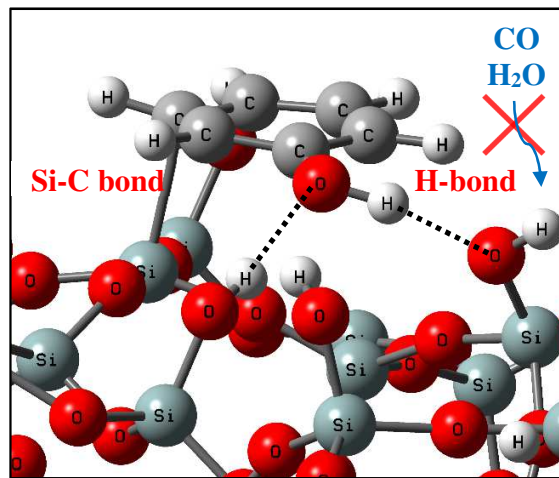
- [1] The promotion of the Use of Biofuels or Related Other Renewable Fuels for Transport., (2003).
- [2] JE. Holladay, JJ. Bozell, JF. White, D. Johnson, Top Value-Added Chemicals from Biomass, PACIFIC NORTHWEST NATIONAL LABORATORY operated by BATTELLE for the UNITED STATES DEPARTMENT OF ENERGY, 2007.
- [3] J. van Haveren, E.L. Scott, J. Sanders, Bulk chemicals from biomass, *Biofuels Bioprod. Biorefining*. 2 (2008) 41–57.
- [4] J.B. Binder, M.J. Gray, J.F. White, Z.C. Zhang, J.E. Holladay, Reactions of lignin model compounds in ionic liquids, *Biomass Bioenergy*. 33 (2009) 1122–1130.
- [5] E. Furimsky, Catalytic hydrodeoxygenation, *Appl Catal A*. 199(2) (2000) 147–190.
- [6] S. Czernik, A.V. Bridgwater, Overview of Applications of Biomass Fast Pyrolysis Oil, *Energy Fuels*. 18 (2004) 590–598.
- [7] A.V. Bridgwater, G.V.C. Peacocke, Fast pyrolysis processes for biomass, *Renew. Sustain. Energy Rev.* 4 (2000) 1–73.
- [8] G.W. Huber, S. Iborra, A. Corma, Synthesis of Transportation Fuels from Biomass: Chemistry, Catalysts, and Engineering, *Chem. Rev.* 106 (2006) 4044–4098.
- [9] J.H. Marsman, J. Wildschut, P. Evers, S. de Koning, H.J. Heeres, Identification and classification of components in flash pyrolysis oil and hydrodeoxygenated oils by two-dimensional gas chromatography and time-of-flight mass spectrometry, *J. Chromatogr. A*. 1188 (2008) 17–25.
- [10] D.C. Elliott, Historical Developments in Hydroprocessing Bio-oils, *Energy Fuels*. 21 (2007) 1792.
- [11] T.V. Choudhary, C.B. Phillips, Renewable fuels via catalytic hydrodeoxygenation, *Appl. Catal. Gen.* 397 (2011) 1–12.
- [12] Z. He, X. Wang, Hydrodeoxygenation of model compounds and catalytic systems for pyrolysis bio-oils upgrading, *Catal. Sustain. Energy*. 1 (2012).
- [13] M. Saidi, F. Samimi, D. Karimipourfard, T. Nimmanwudipong, B.C. Gates, M.R. Rahimpour, Upgrading of lignin-derived bio-oils by catalytic hydrodeoxygenation, *Energy Env. Sci.* 7 (2014) 103–129.
- [14] Q. Bu, H. Lei, A.H. Zacher, L. Wang, S. Ren, J. Liang, Y. Wei, Y. Liu, J. Tang, Q. Zhang, R. Ruan, A review of catalytic hydrodeoxygenation of lignin-derived phenols from biomass pyrolysis, *Bioresour. Technol.* 124 (2012) 470–477.
- [15] Y. Romero, F. Richard, S. Brunet, Hydrodeoxygenation of 2-ethylphenol as a model compound of bio-crude over sulfided Mo-based catalysts: Promoting effect and reaction mechanism, *Appl. Catal. B Environ.* 98 (2010) 213–223.
- [16] V.N. Bui, D. Laurenti, P. Afanasiev, C. Geantet, Hydrodeoxygenation of guaiacol with CoMo catalysts. Part I: Promoting effect of cobalt on HDO selectivity and activity, *Appl. Catal. B Environ.* 101 (2011) 239–245.

- [17] C.V. Loricera, B. Pawelec, A. Infantes-Molina, M.C. Álvarez-Galván, R. Huirache-Acuña, R. Nava, J.L.G. Fierro, Hydrogenolysis of anisole over mesoporous sulfided CoMoW/SBA-15(16) catalysts, *Catal. Today*. 172 (2011) 103–110.
- [18] R.N. Olcese, M. Bettahar, D. Petitjean, B. Malaman, F. Giovanella, A. Dufour, Gas-phase hydrodeoxygenation of guaiacol over Fe/SiO₂ catalyst, *Appl. Catal. B Environ.* 115–116 (2012) 63.
- [19] H.Y. Zhao, D. Li, P. Bui, S.T. Oyama, Hydrodeoxygenation of guaiacol as model compound for pyrolysis oil on transition metal phosphide hydroprocessing catalysts, *Appl. Catal. Gen.* 391 (2011) 305–310.
- [20] M. Badawi, S. Cristol, J.-F. Paul, E. Payen, DFT study of furan adsorption over stable molybdenum sulfide catalyst under HDO conditions, *Comptes Rendus Chim.* 12 (2009) 754–761.
- [21] M. Badawi, J.F. Paul, S. Cristol, E. Payen, Y. Romero, F. Richard, S. Brunet, D. Lambert, X. Portier, A. Popov, E. Kondratieva, J.M. Goupil, J. El Fallah, J.P. Gilson, L. Mariey, A. Travert, F. Maugé, Effect of water on the stability of Mo and CoMo hydrodeoxygenation catalysts: A combined experimental and DFT study, *J. Catal.* 282 (2011) 155–164.
- [22] M. Badawi, J.-F. Paul, E. Payen, Y. Romero, F. Richard, S. Brunet, A. Popov, E. Kondratieva, J.-P. Gilson, L. Mariey, A. Travert, F. Maugé, Hydrodeoxygenation of Phenolic Compounds by Sulfided (Co)Mo/Al₂O₃ Catalysts, a Combined Experimental and Theoretical Study, *Oil Gas Sci. Technol. – Rev. D’IFP Energ. Nouv.* 68 (2013) 829–840.
- [23] J.-S. Moon, E.-G. Kim, Y.-K. Lee, Active sites of Ni₂P/SiO₂ catalyst for hydrodeoxygenation of guaiacol: A joint XAFS and DFT study, *J. Catal.* 311 (2014) 144–152.
- [24] D. Garcia-Pintos, J. Voss, A.D. Jensen, F. Studt, Hydrodeoxygenation of Phenol to Benzene and Cyclohexane on Rh(111) and Rh(211) Surfaces: Insights from Density Functional Theory, *J. Phys. Chem. C*. 120 (2016) 18529–18537.
- [25] A.M. Verma, N. Kishore, DFT study on gas-phase hydrodeoxygenation of guaiacol by various reaction schemes, *Mol. Simul.* 43 (2017) 141–153.
- [26] C. Bouvier, Y. Romero, F. Richard, S. Brunet, Effect of H₂S and CO on the transformation of 2-ethylphenol as a model compound of bio-crude over sulfided Mo-based catalysts: propositions of promoted active sites for deoxygenation pathways based on an experimental study, *Green Chem.* 13 (2011) 2441.
- [27] H. Weigold, Behaviour of Co-Mo-Al₂O₃ catalysts in the hydrodeoxygenation of phenols, *Fuel*. 61 (1982) 1021–1026.
- [28] E. Laurent, B. Delmon, Study of the hydrodeoxygenation of carbonyl, carboxylic and guaiacyl groups over sulfided CoMo/γ-Al₂O₃ and NiMo/γ-Al₂O₃ catalyst, *Appl. Catal. Gen.* 109 (1994) 97–115.
- [29] E. Laurent, B. Delmon, Influence of water in the deactivation of a sulfided NiMo/γ-Al₂O₃ catalyst during hydrodeoxygenation, *J. Catal.* 146 (1994) 281–291.
- [30] M. Badawi, J.-F. Paul, S. Cristol, E. Payen, Guaiacol derivatives and inhibiting species adsorption over MoS₂ and CoMoS catalysts under HDO conditions: A DFT study, *Catal. Commun.* 12 (2011) 901–905.
- [31] M. Asadieraghi, W.M. Ashri Wan Daud, H.F. Abbas, Heterogeneous catalysts for advanced bio-fuel production through catalytic biomass pyrolysis vapor upgrading: a review, *RSC Adv.* 5 (2015) 22234–22255.
- [32] S. De, B. Saha, R. Luque, Hydrodeoxygenation processes: Advances on catalytic transformations of biomass-derived platform chemicals into hydrocarbon fuels, *Bioresour. Technol.* 178 (2015) 108.
- [33] J. Wildschut, F.H. Mahfud, R.H. Venderbosch, H.J. Heeres, Hydrotreatment of Fast Pyrolysis Oil Using Heterogeneous Noble-Metal Catalysts, *Ind. Eng. Chem. Res.* 48 (2009) 10324–10334.
- [34] M. Ferrari, R. Maggi, B. Delmon, P. Grange, Influences of the Hydrogen Sulfide Partial Pressure and of a Nitrogen Compound on the Hydrodeoxygenation Activity of a CoMo/Carbon Catalyst, *J. Catal.* 198 (2001) 47–55.
- [35] O.I. Şenol, E.-M. Ryymin, T.-R. Viljava, A.O.I. Krause, Effect of hydrogen sulphide on the hydrodeoxygenation of aromatic and aliphatic oxygenates on sulphided catalysts, *J. Mol. Catal. Chem.* 277 (2007) 107–112.

- [36] R.N. Olcese, Valorisation des vapeurs de pyrolyse de lignine par hydrodéoxygénation directe catalysées par le fer, PhD Thesis, Université de Lorraine, 2012.
- [37] R. Olcese, M.M. Bettahar, B. Malaman, J. Ghanbaja, L. Tibavizco, D. Petitjean, A. Dufour, Gas-phase hydrodeoxygenation of guaiacol over iron-based catalysts. Effect of gases composition, iron load and supports (silica and activated carbon), *Appl. Catal. B Environ.* 129 (2013) 528–538.
- [38] A. Popov, E. Kondratieva, J.M. Goupil, L. Mariey, P. Bazin, J.-P. Gilson, A. Travert, F. Maugé, Bio-oils Hydrodeoxygenation: Adsorption of Phenolic Molecules on Oxidic Catalyst Supports, *J. Phys. Chem. C* 114 (2010) 15661–15670.
- [39] S.A. Mian, L.-M. Yang, L.C. Saha, E. Ahmed, M. Ajmal, E. Ganz, A Fundamental Understanding of Catechol and Water Adsorption on a Hydrophilic Silica Surface: Exploring the Underwater Adhesion Mechanism of Mussels on an Atomic Scale, *Langmuir*. 30 (2014) 6906–6914.
- [40] S. Simonetti, A.D. Compañy, E. Pronsato, A. Juan, G. Brizuela, A. Lam, Density functional theory based-study of 5-fluorouracil adsorption on β -cristobalite (111) hydroxylated surface: The importance of H-bonding interactions, *Appl. Surf. Sci.* 359 (2015) 474–479.
- [41] A.D. Compañy, A. Juan, G. Brizuela, S. Simonetti, 5-fluorouracil adsorption on hydrated silica: density functional theory based-study, *Adsorption*. 23 (2017) 321–325.
- [42] A. Rimola, B. Civalleri, P. Ugliengo, Physisorption of aromatic organic contaminants at the surface of hydrophobic/hydrophilic silica geosorbents: a B3LYP-D modeling study, *Phys. Chem. Chem. Phys.* 12 (2010) 6357.
- [43] S. Simonetti, A.D. Compañy, G. Brizuela, A. Juan, β -Cristobalite (001) surface as 4-formaminoantipyrine adsorbent: First principle study of the effect on adsorption of surface modification, *Colloids Surf. B Biointerfaces*. 148 (2016) 287–292.
- [44] E.N. Grau, G. Román, A.D. Compañy, G. Brizuela, A. Juan, S. Simonetti, Surface modification vs sorption strength: Study of nedaplatin drug supported on silica, *Appl. Surf. Sci.* 465 (2019) 693–699.
- [45] S. Cristol, J. Paul, C. Schovsbo, E. Veilly, E. Payen, DFT study of thiophene adsorption on molybdenum sulfide, *J. Catal.* 239 (2006) 145–153.
- [46] P.G. Moses, B. Hinnemann, H. Topsøe, J.K. Nørskov, The effect of Co-promotion on MoS₂ catalysts for hydrodesulfurization of thiophene: A density functional study, *J. Catal.* 268 (2009) 201–208.
- [47] F. Pelardy, A. Daudin, E. Devers, C. Dupont, P. Raybaud, S. Brunet, Deep HDS of FCC gasoline over alumina supported CoMoS catalyst: Inhibiting effects of carbon monoxide and water, *Appl. Catal. B Environ.* 183 (2016) 317–327.
- [48] A. Comas-Vives, Amorphous SiO₂ surface models: energetics of the dehydroxylation process, strain, ab initio atomistic thermodynamics and IR spectroscopic signatures, *Phys. Chem. Chem. Phys.* 18 (2016) 7475–7482.
- [49] J. Handzlik, J. Ogonowski, Structure of Isolated Molybdenum(VI) and Molybdenum(IV) Oxide Species on Silica: Periodic and Cluster DFT Studies, *J. Phys. Chem. C* 116 (2012) 5571–5584.
- [50] X. Rozanska, F. Delbecq, P. Sautet, Reconstruction and stability of β -cristobalite 001, 101, and 111 surfaces during dehydroxylation, *Phys. Chem. Chem. Phys.* 12 (2010) 14930.
- [51] T.P.M. Goumans, A. Wander, W.A. Brown, C.R.A. Catlow, Structure and stability of the (001) α -quartz surface, *Phys Chem Chem Phys.* 9 (2007) 2146–2152.
- [52] A. Abbasi, E. Nadimi, P. Plänitz, C. Radehaus, Density functional study of the adsorption of aspirin on the hydroxylated (001)-quartz surface, *Surf. Sci.* 603 (2009) 2502–2506.
- [53] P. Hohenberg, W. Kohn, Inhomogeneous Electron Gas, *Phys. Rev.* 136 (1964) B864–B871.
- [54] W. Kohn, L.J. Sham, Quantum Density Oscillations in an Inhomogeneous Electron Gas, *Phys. Rev.* 137 (1965) A1697–A1705.
- [55] G. Kresse, J. Hafner, *Ab initio* molecular dynamics for liquid metals, *Phys. Rev. B*. 47 (1993) 558.
- [56] G. Kresse, J. Hafner, *Ab initio* molecular-dynamics simulation of the liquid-metal–amorphous-semiconductor transition in germanium, *Phys. Rev. B*. 49 (1994) 14251–14269.

- [57] J.P. Perdew, K. Burke, M. Ernzerhof, Generalized Gradient Approximation Made Simple, *Phys. Rev. Lett.* 77 (1996) 3865–3868.
- [58] G. Kresse, J. Furthmüller, Efficient iterative schemes for *ab initio* total-energy calculations using a plane-wave basis set, *Phys. Rev. B.* 54 (1996) 11169–11186.
- [59] G. Kresse, D. Joubert, From ultrasoft pseudopotentials to the projector augmented-wave method, *Phys. Rev. B.* 59 (1999) 1758–1775.
- [60] T. Sun, Y. Wang, H. Zhang, P. Liu, H. Zhao, Adsorption and oxidation of oxalic acid on anatase TiO₂ (001) surface: A density functional theory study, *J. Colloid Interface Sci.* 454 (2015) 180–186.
- [61] A. Tkatchenko, M. Scheffler, Accurate Molecular Van Der Waals Interactions from Ground-State Electron Density and Free-Atom Reference Data, *Phys. Rev. Lett.* 102 (2009) 073005.
- [62] T. Bučko, J. Hafner, S. Lebègue, J.G. Ángyán, Improved Description of the Structure of Molecular and Layered Crystals: Ab Initio DFT Calculations with van der Waals Corrections, *J. Phys. Chem. A.* 114 (2010) 11814–11824.
- [63] F. Göttl, A. Grüneis, T. Bučko, J. Hafner, Van der Waals interactions between hydrocarbon molecules and zeolites: Periodic calculations at different levels of theory, from density functional theory to the random phase approximation and Møller-Plesset perturbation theory, *J. Chem. Phys.* 137 (2012) 114111.
- [64] T. Bučko, S. Lebègue, J. Hafner, J.G. Ángyán, Improved Density Dependent Correction for the Description of London Dispersion Forces, *J. Chem. Theory Comput.* 9 (2013) 4293–4299.
- [65] T. Bučko, S. Lebègue, J.G. Ángyán, J. Hafner, Extending the applicability of the Tkatchenko-Scheffler dispersion correction via iterative Hirshfeld partitioning, *J. Chem. Phys.* 141 (2014) 034114.
- [66] U. Zimmerli, M. Parrinello, P. Koumoutsakos, Dispersion corrections to density functionals for water aromatic interactions, *J. Chem. Phys.* 120 (2004) 2693–2699.
- [67] M. Dion, H. Rydberg, E. Schröder, D.C. Langreth, B.I. Lundqvist, Van der Waals Density Functional for General Geometries, *Phys. Rev. Lett.* 92 (2004) 246401.
- [68] S. Grimme, Accurate description of van der Waals complexes by density functional theory including empirical corrections, *J. Comput. Chem.* 25 (2004) 1463–1473.
- [69] S. Grimme, Semiempirical GGA-type density functional constructed with a long-range dispersion correction, *J. Comput. Chem.* 27 (2006) 1787–1799.
- [70] S. Grimme, J. Antony, S. Ehrlich, H. Krieg, A consistent and accurate ab initio parametrization of density functional dispersion correction (DFT-D) for the 94 elements H-Pu, *J. Chem. Phys.* 132 (2010) 154104.
- [71] S. Grimme, S. Ehrlich, L. Goerigk, Effect of the damping function in dispersion corrected density functional theory, *J. Comput. Chem.* 32 (2011) 1456–1465.
- [72] J. Yang, S. Meng, L. Xu, E.G. Wang, Water adsorption on hydroxylated silica surfaces studied using the density functional theory, *Phys. Rev. B.* 71 (2005).
- [73] J. Yang, E.G. Wang, Water adsorption on hydroxylated α -quartz (0001) surfaces: From monomer to flat bilayer, *Phys. Rev. B.* 73 (2006).
- [74] V.A. Bakaev, W.A. Steele, On the computer simulation of a hydrophobic vitreous silica surface, *J. Chem. Phys.* 111 (1999) 9803–9812.
- [75] E.A. Leed, C.G. Pantano, Computer modeling of water adsorption on silica and silicate glass fracture surfaces, *J. Non-Cryst. Solids.* 325 (2003) 48–60.

Graphical Abstract



High adsorption selectivity of phenol vs CO and H₂O on amorphous silica